

Yellow fever vaccine induces integrated multilineage and polyfunctional immune responses

Denis Gaucher,^{1,2,3} René Therrien,^{1,2,3} Nadia Kettaf,^{1,2,3}
 Bastian R. Angermann,^{1,2} Geneviève Boucher,¹ Abdelali Filali-Mouhim,¹
 Janice M. Moser,⁴ Riyaz S. Mehta,⁴ Donald R. Drake III,⁴ Erika Castro,^{5,6}
 Rama Akondy,⁷ Aline Rinfret,^{8,9} Bader Yassine-Diab,^{1,2,3} Elias A. Said,^{1,2,3}
 Younes Chouikh,^{1,2,3} Mark J. Cameron,¹⁰ Robert Clum,¹⁰ David Kelvin,¹⁰
 Roland Somogyi,¹¹ Larry D. Greller,¹¹ Robert S. Balderas,¹²
 Peter Wilkinson,¹ Giuseppe Pantaleo,⁵ Jim Tartaglia,¹³
 Elias K. Haddad,^{1,2,3,14} and Rafick-Pierre Sékaly^{1,2,3,14}

¹Laboratoire d'immunologie, Centre de Recherche du Centre Hospitalier de l'Université de Montréal (CR-CHUM) Saint-Luc, Montréal, Québec, H2X 1P1, Canada

²Laboratoire d'immunologie, Département de microbiologie et d'immunologie, ³INSERM U743, CR-CHUM, Université de Montréal, Québec H2X 1P1, Canada

⁴VaxDesign Corporation, Orlando, FL 32826

⁵Division of Immunology and Allergy, Department of Medicine, Centre Hospitalier Universitaire Vaudois, University of Lausanne, 1011 Lausanne, Switzerland

⁶Travel Medicine and Vaccination Unit, Polyclinique Médicale Universitaire, 1011 Lausanne, Switzerland

⁷Emory Vaccine Center, Emory University School of Medicine, Atlanta, GA 30322

⁸Canadian Network for Vaccines and Immunotherapeutics, Montréal, Québec, H3X 2H9, Canada

⁹Biologics and Genetic Therapies Directorate, Health Canada, Tunney's Pasture, Ottawa, Ontario, K1A 0K9, Canada

¹⁰Toronto General Research Institute, University Health Network, Toronto, Ontario M5G 2M9, Canada

¹¹Biosystemix, Ltd., Sydenham, Ontario K0H 2T0, Canada

¹²BD Biosciences, San Diego, CA 92121

¹³Aventis Pasteur, Ltd., Toronto, Ontario, M2R 3T4, Canada

¹⁴Department of Microbiology and Immunology, McGill University, Montréal, Québec, H3A 2B4, Canada

Correlates of immune-mediated protection to most viral and cancer vaccines are still unknown. This impedes the development of novel vaccines to incurable diseases such as HIV and cancer. In this study, we have used functional genomics and polychromatic flow cytometry to define the signature of the immune response to the yellow fever (YF) vaccine 17D (YF17D) in a cohort of 40 volunteers followed for up to 1 yr after vaccination. We show that immunization with YF17D leads to an integrated immune response that includes several effector arms of innate immunity, including complement, the inflammasome, and interferons, as well as adaptive immunity as shown by an early T cell response followed by a brisk and variable B cell response. Development of these responses is preceded, as demonstrated in three independent vaccination trials and in a novel *in vitro* system of primary immune responses (modular immune *in vitro* construct [MIMIC] system), by the coordinated up-regulation of transcripts for specific transcription factors, including STAT1, IRF7, and ETS2, which are upstream of the different effector arms of the immune response. These results clearly show that the immune response to a strong vaccine is preceded by coordinated induction of master transcription factors that lead to the development of a broad, polyfunctional, and persistent immune response that integrates all effector cells of the immune system.

CORRESPONDENCE
 Rafick-Pierre Sékaly:
 rafick-pierre.sekaly@umontreal.ca

Abbreviations used: CBA, cyto-metric bead assay; ICA, independent component analysis; MIMIC, modular immune *in vitro* construct; qPCR, quantitative real-time PCR; TLR, Toll-like receptor; YF, yellow fever; YF17D, YF vaccine 17D.

N. Kettaf and B.R. Angermann and E.K. Haddad and R.-P. Sékaly contributed equally to this paper.

© 2008 Gaucher et al. This article is distributed under the terms of an Attribution-Noncommercial-Share Alike-No Mirror Sites license for the first six months after the publication date (see <http://www.jem.org/misc/terms.shtml>). After six months it is available under a Creative Commons License (Attribution-Noncommercial-Share Alike 3.0 Unported license, as described at <http://creativecommons.org/licenses/by-nc-sa/3.0/>).

Correlates of immune-mediated protection to most viral and cancer vaccines are still unknown. Moreover, there is a paucity of information regarding the qualitative and quantitative properties of emerging protective responses *in vivo* in humans, and this has been a major impediment to vaccine development (1). Although humoral immunity is clearly the dominant correlate of protection for vaccines against bacterial pathogens (2), viruses or tumors require a more complex immune response with contributions from both T and B cells (3). Innate immunity, which is known to shape the development of adaptive immune responses, could also contribute to vaccine-mediated protection through mechanisms yet to be defined.

Developed empirically in the 1930s, the live attenuated yellow fever (YF) vaccine 17D (YF17D) is considered one of the most successful vaccines ever made (4); a single dose can confer protective immunity for up to 35 yr, in almost all vaccinated individuals. The humoral immune response to 17D is generally considered the main mediator of protection against a challenge infection with wild-type YF virus. Passive immunization in monkeys (5) and mice (6) has mediated protection against YF infection. Although the humoral response inarguably plays a central role, we cannot rule out the contribution of the other arms of the immune system, cellular and innate immunity, as help from CD4⁺ T cells is needed to generate a strong B cell response. With the disease being caused by a virus, and the vaccine itself being an attenuated virus, one could expect cytotoxic T cells to play a crucial role in destroying virally infected cells, and thus preventing viral replication and spreading. Surprisingly, there is very little published data on the cellular response to the YF17D vaccine in humans. The kinetics of the levels of total CD4⁺ and CD8⁺ T cells (7) and nonspecific memory CD4⁺ and CD8⁺ T cells (8) after vaccination were initially studied, and the first study of YF17D antigen-specific T cells came from Co et al., who mapped a series of HLA-B35-restricted CD8⁺ epitopes to the envelope, NS1, NS2b, and NS3 proteins (9). Miller et al. recently described the kinetics and properties of the antigen-specific CD8⁺ T cell memory response after YF17D vaccination (10).

The identification of correlates of protection to YF, however useful it will be, is destined to be difficult. Classical studies where vaccinated subjects are challenged with a virulent, wild-type strain can obviously not be performed on humans. Therefore, we have to rely on data derived from vaccination campaigns performed in populations living in endemic areas or among high-risk people. Furthermore, the vaccine's high efficacy makes it nearly impossible to identify individuals who did not acquire protective immunity from it, and it is virtually impossible to study such subjects. For these reasons, we have to develop and rely on other parameters that can indicate the strength of the immune response induced in the vaccinated individuals, such as the level of viremia, the neutralizing antibody titers, or the breadth of the cellular immune response.

Herein, we have used a systems biology approach combined with multiparametric flow cytometry and a novel *in vitro* system of primary immune responses (VaxDesign's modular

immune *in vitro* construct [MIMIC] co-culture system), to identify the emerging protective immune response induced in humans by vaccination with YF17D, in an effort to unravel the correlates of protection conferred by one of the most potent vaccines ever generated.

RESULTS

Vaccination with YF17D rapidly and transiently induces modulation of genes associated with multiple pathways

RNA samples obtained from whole blood of 15 YF17D-vaccinated individuals (from the Montreal cohort) on the day of vaccination (day 0) and at several time points after vaccination (day 3, 7, 10, 14, 28, and 60) were amplified and hybridized onto Illumina chips and analyzed. Expression profiles of 594 genes (Supplemental document 1, available at <http://www.jem.org/cgi/content/full/jem.20082292/DC1>) were found to change significantly between day 0 and any time point after vaccination (with $P < 0.05$ and fold change less than -1.3 or >1.3). The peak of modulation of gene expression, as shown by heat map representation (Fig. 1 a) and principal component analysis (Fig. 1 b), primarily occurred at days 3 and 7 after vaccination, whereas a limited number of significant genes were modulated in response to vaccination at day 10 after vaccination or beyond.

Independent component analysis (ICA), followed by gene set enrichment, identified transcription factors with predicted (11) target genes showing a specific modulation after YF17D vaccination (Fig. 2 and Fig. S1, available at <http://www.jem.org/cgi/content/full/jem.20082292/DC1>). With this approach, three major nodes of transcriptional regulation

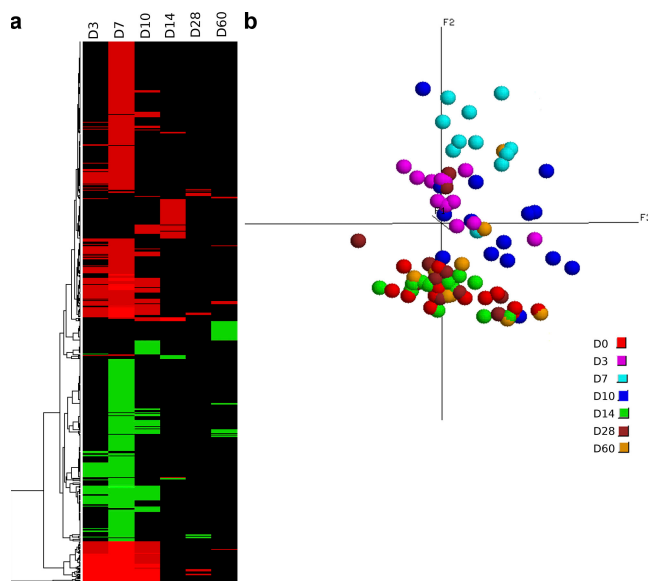


Figure 1. Vaccination with YF17D induces early gene modulation. Global view of gene modulation in total blood cells after YF17D vaccination, as analyzed by gene array on the Montreal cohort ($n = 9-15$, depending on the time point). Heat map representation (a) and PCA (b) using the significantly modulated genes, in at least one comparison versus day 0.

of downstream target genes were found as early as day 3 (IRF7 and STAT1) and day 7 (ETS2). Other nodes of transcription factors (IRF1, IRF8, GATA6, GATA1, TAL1, FOXO3a, E2F4, E2F1, LMO2, SRF, and CEBPB) also controlled the expression of several of the genes and pathways that were modulated in the first week after immunization.

Many of the genes that were modulated by YF17D vaccination could be classified under different functional categories, based on published literature (Fig. 3 and Supplemental document 2, available at <http://www.jem.org/cgi/content/full/jem.20082292/DC1>). Some Toll-like receptor (TLR)-associated genes (TLR7, MYD88, and IRF7) were also up-regulated, leading to the activation of the IFN pathway, as monitored by the induction of several IFN-induced genes (IFI27, IFI30, G1P2, G1P3, and OAS1-3; Fig. 3 a and Supplemental document 1). Components of the complement system (C1QA, C1QB, C3AR1, and SERPING1) were found to be up-regulated in blood cells early after vaccination (Fig. 3 b). A few macrophage/DC-associated genes were induced significantly by the vaccine, including CD86 (a marker of DC maturation), CSF1R, MARCO, and IFI16, which are expressed by cells of the monocyte-macrophage lineage (Fig. 3 c). NK cell-associated genes (KIR2DL3, KIR2DL4, PRF1, GNLY, and GZMB) were also up-regulated (Fig. 3 d).

Genes associated with B cell activation (BANK1, CD19, IGJ, TNFRSF13B, and TNFRSF17l; Fig. 3 e) were also modulated. Other genes also involved in the induction of an immune response, such as TAP1 and TAP2, which encode proteins involved in antigen processing and presentation (12, 13), and SOCS1, which encodes a protein involved in a negative feedback loop meant to attenuate cytokine signaling (14), were up-regulated as well (Supplemental document 1). Strikingly, we observed that 43 genes encoding ribosomal proteins were down-regulated in PBMCs early after vaccination with YF17D (Supplemental document 1), confirming the findings of a previous study (15). Collectively, these results reveal that vaccination with YF17D stimulated a rapid and transient modulation of several genes of immunological importance, which allowed us to infer a signature of gene modulation by ICA.

Two levels of validation were performed to confirm the results observed in this initial trial; the first validation was achieved by performing quantitative real-time PCR (qPCR) on RNA from 7 volunteers from the Montreal cohort for 43 genes selected to represent 8 of the identified transcription nodes and some of their target genes. As shown in Fig. S2 (available at <http://www.jem.org/cgi/content/full/jem.20082292/DC1>), we could observe a highly significant correlation between the results obtained by qPCR and those

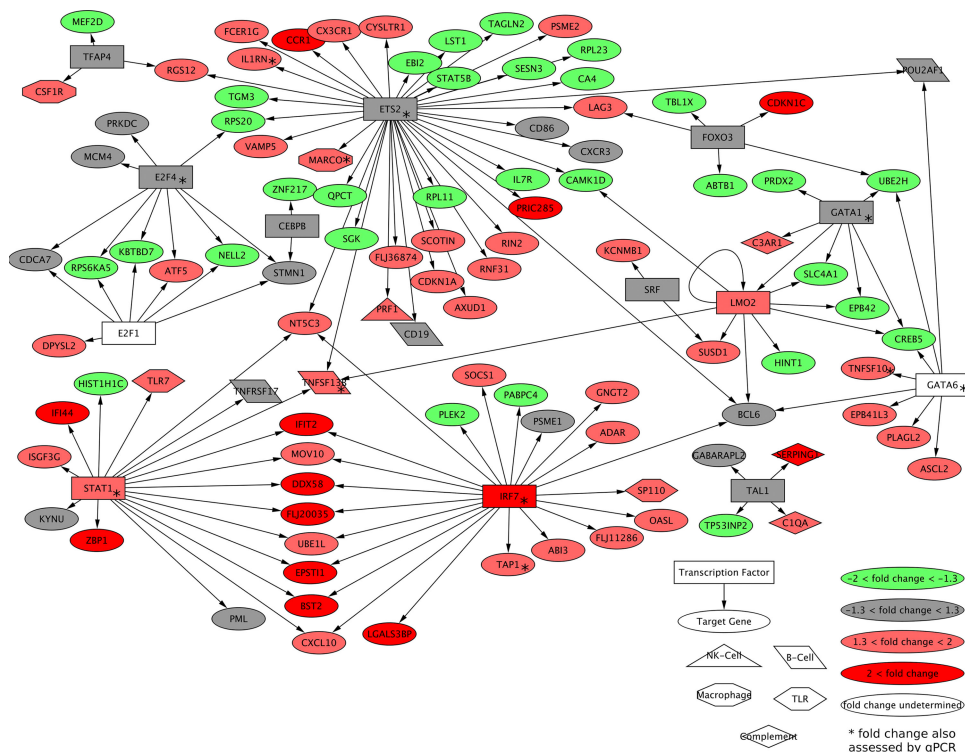


Figure 2. Transcriptional network of differentially expressed genes after YF17D vaccination, as inferred by gene set enrichment. Network representation of inferred transcription factors (11) and predicted target genes that are significantly modulated. Node colors indicate fold change of gene expression between day 0 and 7 in $n = 11$ volunteers. Rectangular nodes indicate transcription factors identified by gene enrichment; the different shapes indicate genes in the different functional categories of Fig. 3 (a–e). Genes that were subsequently evaluated by RT-PCR are identified by an asterisk. IRF1, IRF8, and genes targeted by IRF1 or IRF8, but no other transcription factors in the figure were removed to increase readability (see Fig. S1 for a complete map). Fig. S1 is available at <http://www.jem.org/cgi/content/full/jem.20082292/DC1>.

obtained by gene microarray, with coefficients of correlation ranging between 0.78 and 0.96. A detailed analysis of the entire set of genes is represented in Table S1. The second validation was achieved by comparing the aforementioned qPCR dataset for the Montreal cohort to datasets from two other, independent YF17D vaccination trials: the Lausanne cohort (13 volunteers) and the Emory cohort (10 volunteers). The results illustrated in Fig. 4 and in Fig. S3 indicate that most genes that were up-regulated in the Montreal cohort also showed increased expression in the two other independent trials. Conversely, most down-regulated genes in the Montreal cohort also showed decreased levels of expression in the samples obtained from the two other trials. These results demonstrate the proper validation of our gene array data by two different strategies: the use of qPCR and an increase in sample size.

The YF17D vaccine up-regulates IL-1 β production

Our gene array results showed that two components of the inflammasome, caspase-1 and -5, were up-regulated at the mRNA level in the Montreal cohort, 3 d after vaccination with YF17D (Fig. 5 a). Two other genes related to IL-1 β production and signaling that were modulated by the vaccine are IL-1R2 and -1RN. All of these genes, except for caspase-5, were also similarly modulated in the Lausanne cohort. To functionally validate the microarray data suggesting the acti-

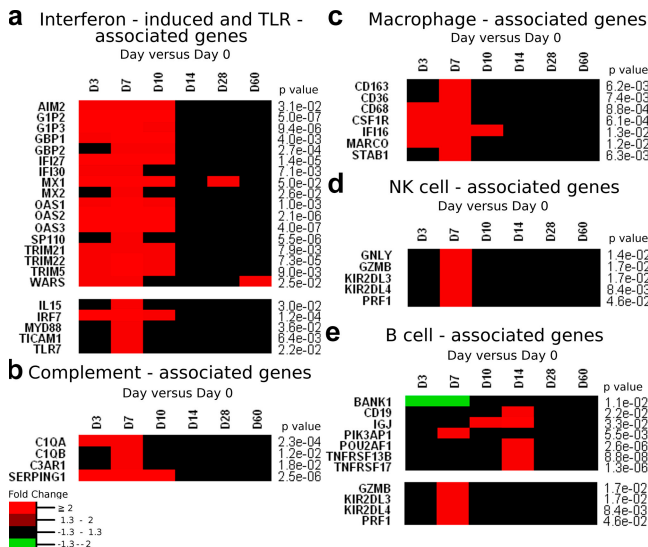


Figure 3. YF17D vaccination stimulates multiple arms of the innate and adaptive immunity. (a–e) Heat map representation of significantly modulated genes, P values listed with each gene indicate the largest (least significant) P value among the significant fold changes. $n = 9$ –15, depending on the time point. The listed genes fall under different functional categories: IFN-induced and TLR-associated genes (a); complement-associated genes (b); macrophage-associated genes (c); NK cell-associated genes (d); and B cell-associated genes (e). Supplemental document 2 includes a justification for the attribution of each gene into its respective group. Supplemental document 2 is available at <http://www.jem.org/cgi/content/full/jem.20082292/DC1>.

vation of the inflammasome by the vaccine, we quantified the secretion of IL-1 β , which has been shown to be processed and produced by an active inflammasome assembly (16). The results show that DCs incubated with live or UV-inactivated YF17D showed a marked increased IL-1 β secretion (up to ninefold, compared with DCs incubated in medium alone), whereas heat-inactivated YF17D only triggered a modest secretion of the proinflammatory cytokine (Fig. 5 b and Fig. S4, available at <http://www.jem.org/cgi/content/full/jem.20082292/DC1>). These functional results confirm the gene array data, suggesting that YF17D activates components of the inflammasome complex, and that viral replication is not required for this effect.

YF17D vaccination leads to the proliferation and expansion of several leukocyte subtypes

Given that immunization with YF17D gives rise to the up-regulation of genes associated with different leukocyte populations, we were interested in determining whether the vaccine also induces the proliferation of these cells. To do so, PBMCs from 6 volunteers, sampled at day 0, 3, 7, 10, 14, and 28 after vaccination, were stained with anti-Ki67 and other specific antibodies to identify, by flow cytometry, different cell subsets that are actively proliferating. The staining/gating strategies and the results are shown in Fig. S5 (a and b, available at <http://www.jem.org/cgi/content/full/jem.20082292/DC1>), respectively. An increase in frequencies of Ki67 $^+$ cells in the CD4 $^+$ CD8 $^-$ (2.3-fold increase; $P = 0.0049$) and the CD4 $^-$ CD8 $^+$ (4.7-fold increase; $P = 0.0157$) populations occurred within the first 14 d after YF17D vaccination, and then decreased to insignificant levels. The Ki67 $^+$ NK cell population

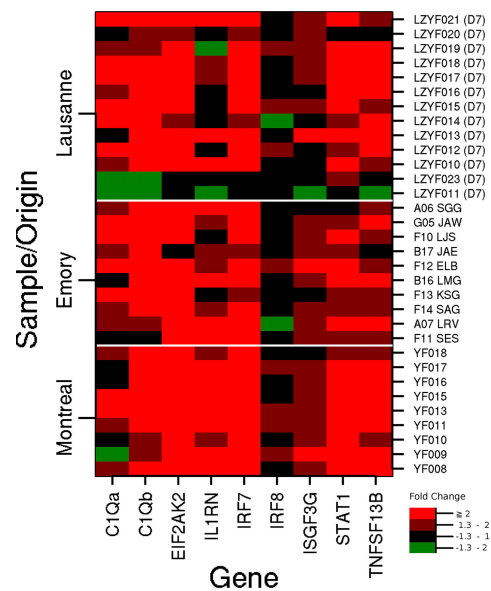


Figure 4. Heat map of fold change gene expression between day 0 and 7, as measured by qPCR. For a complete heat map of all measured fold changes see Fig. S3. Fig. S3 is available at <http://www.jem.org/cgi/content/full/jem.20082292/DC1>.

(CD3⁻CD8^{Dim}, 1.6-fold; $P = 0.0474$) and non-T cell PBMCs containing monocytes and B cells (CD3⁻CD4⁻CD8⁻; 1.9-fold; $P = 0.009$) also increased in frequency within the first 7 d and reached insignificant levels thereafter. Altogether, our data clearly illustrate that all major cellular subsets of innate and adaptive immunity are mobilized during the immune response to YF17D.

Vaccination with YF17D induces a broad and persistent YF-specific T cell response

We next assessed the amplitude, breadth, and persistence of the YF17D-specific T cell response. PBMCs sampled at day 60 after vaccination were incubated in the presence of each of 22 YF17D-derived peptide pools (Fig. S6 a, available at <http://www.jem.org/cgi/content/full/jem.20082292/DC1>), and their proliferation was measured by CFSE labeling. Fig. S6 b describes the cytometry gating strategy used, and the results are shown in Fig. 6 (bar graphs) and Fig. S6 (c and d). Both the CD4⁺ and CD8⁺ T cell proliferative responses were highly variable among the vaccinated volunteers. Strong CD4⁺ responders (notably YF001, 002, 009, 018, and 020) recognized

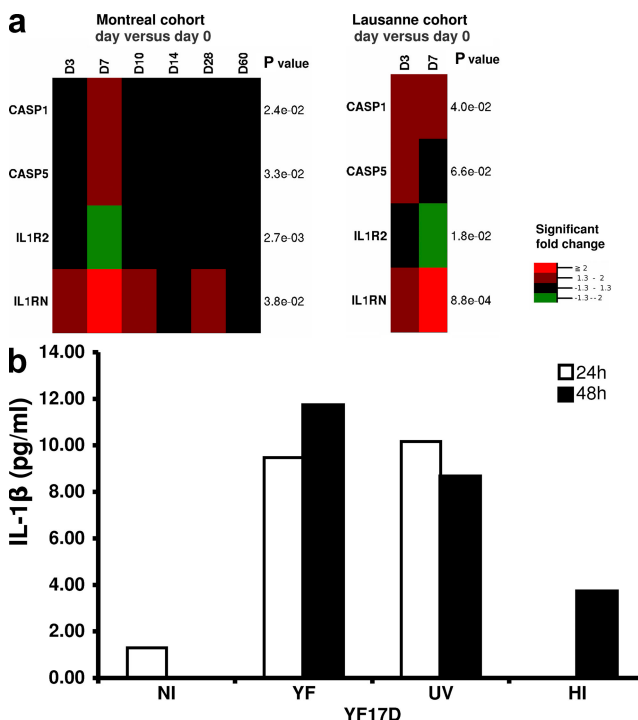


Figure 5. YF17D induces expression of genes associated with IL-1 β and activates the inflammasome. (a) Heat maps showing the up-regulation of genes encoding inflammasome components and the modulation of other, IL-1 β -associated genes. For IL-1R2 and -1RN only probes targeting all transcripts were considered. (b) IL-1 β production by monocyte-derived DCs incubated with live (YF), UV-inactivated (UV), or heat-inactivated (HI) YF17D, as determined by ELISA. NI, noninfected cells. This represents the results from one representative of three separate experiments. The results for the two other experiments are shown in Fig. S4. Fig. S4 is available at <http://www.jem.org/cgi/content/full/jem.20082292/DC1>.

most, if not all, of the peptide pools (>20), whereas weak responders (YF005, 011, and 017) recognized only a few (<5). The CD8⁺ responses were generally much weaker than those observed in CD4⁺ T cells, and although only 2 responders recognized 19 of the pools (YF001 and 020), 10 of them recognized <5 . Notably, some peptide pools were recognized by more volunteers than others (pools 1, 3, and 17 were recognized by CD4⁺ T cells of at least 12 volunteers), whereas others were recognized by just a few volunteers (pools 5 and 7 were recognized by CD4⁺ cells of at most 7 volunteers). Both CD4⁺ and CD8⁺ T cell peptide-specific responses were persistent, as memory proliferative responses to the most immunodominant peptide pools were detected as long as 1 yr after immunization (unpublished data). These results show that the breadth of the T cell responses to the YF17D vaccine is highly variable from one vaccinated individual to another, but that those responses are persistent.

The YF17D vaccine induces a mixed Th1/Th2 response that appears early and is persistent

Next, we sought to determine at the protein level the cytokine profiles produced by PBMCs after stimulation with YF17D-derived peptide pools. We used cytometric bead assay (CBA) to assess the levels of the Th1 cytokines IL-2, IFN- γ , and TNF, and the Th2 cytokines IL-4 and -10 secreted by these cells. Fig. 6 shows the results for six selected volunteers (heat maps); a summary of the CBA results for all volunteers and pools tested can be found in Fig. S6 e. In our system, high levels of TNF were detected in several supernatants, whereas the other cytokines were either found in low amounts or not detected. Hence, the qualitative and quantitative features of cytokine production were highly variable; pool 3 stimulated a mixed Th1/Th2 response in volunteer YF001, but triggered only a Th1 response in subjects YF002, 3, 9, and 20, whereas no detectable response to this pool could be seen in YF019. In most volunteers (12 out of 15), both Th1 and Th2 cytokine secretion profiles were induced by YF17D peptide pools. Three volunteers (YF0014, 15, and 16), who were weak responders to the vaccine as measured by T cell proliferation, did not show a mixed Th1/Th2 profile; however, these individuals were still able to mount very good antibody responses (Table S2, available at <http://www.jem.org/cgi/content/full/jem.20082292/DC1>).

We further demonstrated the emergence of a mixed Th1/Th2 response to the vaccine at the single-cell level using polychromatic flow cytometry. First, we confirmed the Th1 phenotype of antigen-specific CD4⁺ T cells by stimulating PBMCs from vaccinated volunteers (28 d after vaccination) with immunostimulatory peptide pools, and identifying antigen-specific T cells by the expression of the activation marker CD154 (17, 18) and the production of IL-2 and IFN- γ . As illustrated in Fig. 7 a, 35.2% of CD4⁺CD154⁺ cells expressed IL-2 alone, 8.6% expressed IFN- γ alone, and 29.5% expressed both IL-2 and IFN- γ .

To determine if this mixed Th1/Th2 response was persistent, we detected YF17D-specific Th1 and Th2 cells in

PBMCs sampled at day 365 after vaccination. The cells were stimulated for 6 d with YF17D-derived immunostimulatory peptide pools to increase the frequency of antigen-specific cells, and then restimulated with the same pools for 18 h. The cells were then stained for the activation marker CD154, as well as for surface markers, allowing the discrimination between the Th1 ($\text{CXCR3}^+ \text{CCR4}^-$) and Th2 ($\text{CXCR3}^- \text{CCR4}^+ \text{CCR6}^-$) phenotypes in central memory T helper cells (19). See Fig. S7 (available at <http://www.jem.org/cgi/content/full/jem.20082292/DC1>) for the full staining and gating strategies and Fig. 7 b for the results. Although some peptide pools stimulated a mixed Th1/Th2 response in a given volunteer, others either stimulated a Th1, a Th2, or no particular profile. However, both Th1 and Th2 cen-

tral memory T cells could be detected in all four volunteers tested. Together, these results confirm the polyfunctionality of the immune response induced by YF17D, as we observe not only a strong innate immune response but also a mixed Th1/Th2 response that is persistent.

The transcription factors identified during in vivo YF17D vaccination were also central in an in vitro model of YF17D primary immune response

The MIMIC system is a powerful tool for the in vitro study of the early events taking place in a primary immune response. We used this novel approach to validate the multilineage response to YF17D, particularly the expression of transcription nodes and the secretion of mixed Th1/Th2 cytokines. Blood

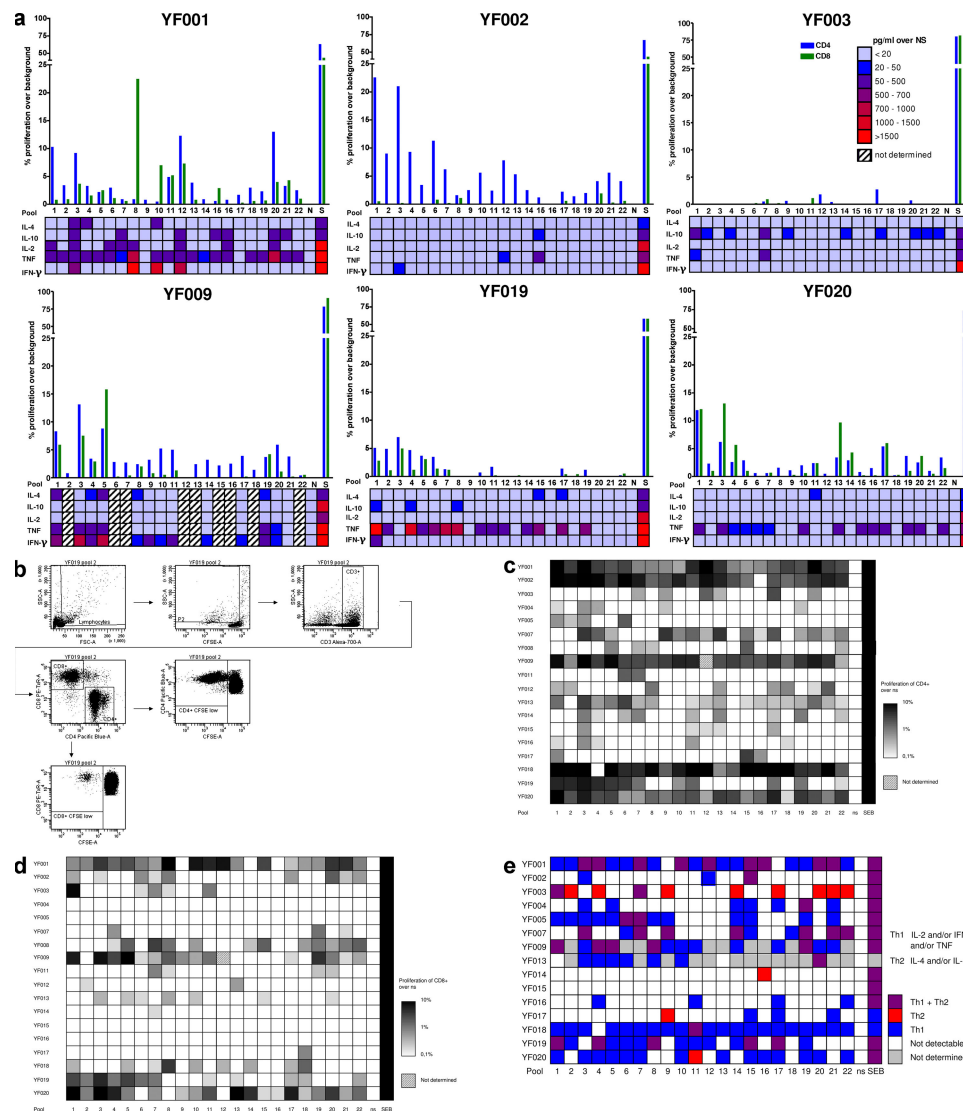


Figure 6. YF17D induces a mixed Th1/Th2 response. (a) Day 60 PBMCs were stimulated with the 22 peptide pools and assayed by CFSE labeling for their proliferative response. Bar graphs show data for six selected volunteers, and the dataset for all the volunteers can be found in Fig. S6 (c and d). At 24 h of culture, supernatants were analyzed by CBA to determine the Th1/Th2 cytokine secretion profile in response to each pool. The heat maps represent the data for the same six volunteers. The Th1/Th2 profiles determined this way for all the volunteers and pools are shown in Fig. S6 e. Fig. S6 is available at <http://www.jem.org/cgi/content/full/jem.20082292/DC1>.

monocyte-derived DCs from YF-naive individuals were pulsed with YF17D virus for 24 h, and then co-cultured for 14 d with autologous CD4⁺ T cells. The resulting culture superna-

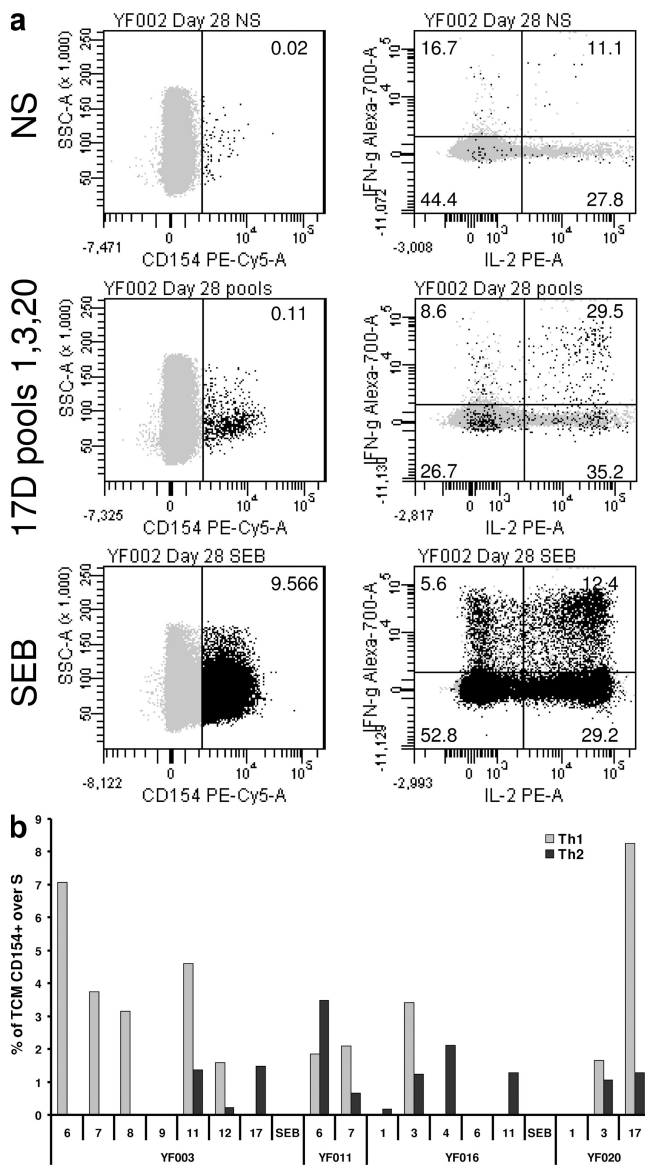


Figure 7. YF17D vaccination induces specific CD4⁺ T cells of mixed T helper phenotype. (a) PBMCs from YF17D-vaccinated volunteers (day 28 after vaccination) were stimulated with a group of three immunostimulatory YF17D-derived peptide pools, and then stained with antibodies against CD4 (surface) and CD154, IL-2, and IFN- γ (intracellular). The numbers indicate the percentages of cells within the parent population. (b) FACS analysis of PBMCs from day 365 after vaccination. Cells from four volunteers were stimulated (S) for with immunostimulatory YF17D peptide pools, and then restimulated (RS) or not with the same peptide pools before staining. The data were analyzed according to the gating strategy shown in Fig. S7, and are expressed as the percentage of central memory CD4⁺ T cells (CD45RA2CCR7⁺) that express the marker for recent activation CD154, and that are either Th1 or Th2 in the RS samples, over background (S). Fig. S7 is available at <http://www.jem.org/cgi/content/full/jem.20082292/DC1>.

tants were harvested for cytokine quantification, and the cells stained for polychromatic flow cytometry analysis. As shown in Fig. 8 a, DCs pulsed with YF17D virus (live or UV-inactivated) primed a strong antigen-specific response of naive T cells, with up to 4% cells expressing CD154 and IFN- γ in

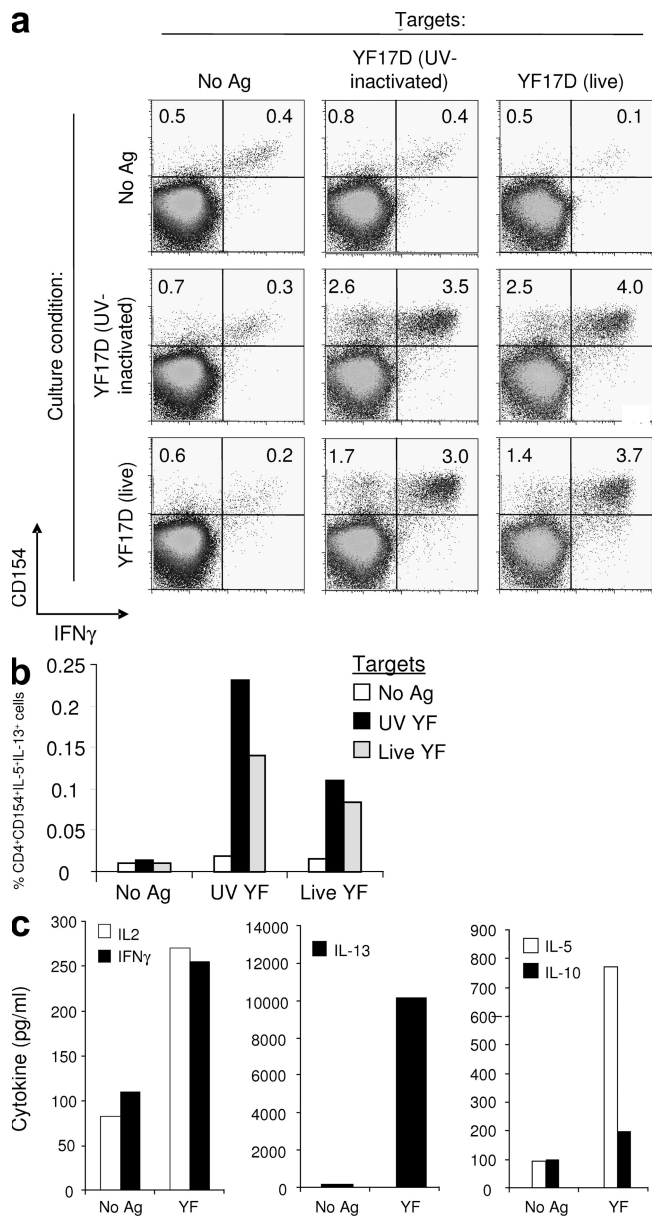


Figure 8. YF17D elicits robust and diverse primary T helper cell responses in DC/T cell co-cultures. (a and b) Purified T helper cells were mixed with DCs that had been incubated with live or UV-inactivated YF17D. After 14 d, the cells were harvested and evaluated by flow cytometry for cytokine and CD154 expression after a short restimulation with autologous DCs targets that had been left untouched, pulsed with killed YF17D, or infected with live YF17D. All data plots show live CD4⁺-gated events. These are representative data of experiments done on cells from at least 10 volunteers. (c) Alternatively, the culture supernatants were harvested and evaluated by a multiplex cytokine analysis. Data representative of experiments done on cells from two volunteers.

response to live or UV-inactivated YF17D. Similarly, YF17D-pulsed DCs stimulated high numbers of antigen-specific Th2 cells expressing IL-5 and IL-13, upon restimulation with live or inactivated virus (Fig. 8 b). The levels of the cytokines IL-2, IFN- γ , IL-13, IL-5, and IL-10 in the MIMIC co-culture supernatants were measured by multiplex cytokine analysis (Fig. 8 c). When YF17D was used as pulse and recall antigen, the cells produced high levels of all the cytokines measured except IL-10, compared with co-cultures with no recall antigen. Collectively, the results show that the MIMIC system induced a YF17D-specific primary CD4 $^{+}$ T cell response, and furthermore, it allowed us to confirm the induction of a mixed Th1/Th2 immune response by the YF17D vaccine.

Finally, the MIMIC approach was used to independently assess our working hypothesis that the transcriptional nodes induced in whole blood cells after vaccination with YF17D can also be induced in vitro by the vaccine. Co-cultures containing YF17D-pulsed DCs and CD4 $^{+}$ T cells (with or without YF17D as recall antigen) were harvested and total RNA was isolated from the cells. Gene modulation in response to the antigen (day 7 vs. 0) was assessed by microarray analysis. In total, eight nodes of transcriptional regulation of downstream target genes were consistently identified; ETS2, STAT1, IRF1, IRF7, IRF8, GATA1, LMO2, and JUN (Fig. 9). Table S3 (available at <http://www.jem.org/cgi/content/full/jem.20082292/DC1>) summarizes the transcriptional nodes identified with the Montreal cohort, the Lausanne cohort, and the VaxDesign system. These data demonstrate that the same central nodes of transcription are activated in vivo vaccination with YF17D and in an in vitro system of primary immune response to the virus.

DISCUSSION

In this study, we have used systems biology and polychromatic flow cytometry to characterize the early immunologi-

cal processes that are initiated by one of the most potent vaccines ever generated, the YF vaccine YF17D, and which culminate into persistent immunological memory and long-term protection against a challenge infection (20). The vaccine induced a significant modulation of 594 genes in whole blood cells, with the highest number of genes being induced at day 7 after vaccination. ICA and gene set enrichment allowed us to identify several nodes of transcriptional regulation that became induced within the first week after immunization. This early response was highly integrated, as several of the downstream target genes were coordinately regulated by these transcription factors.

Of the identified nodes, IRF7 was prominently involved in this masterswitch regulation. The induction of IRF7 has been shown to mediate innate and adaptive immunity against many viruses, including encephalomyocarditis virus, vesicular stomatitis virus, influenza virus, and Sindbis virus (21, 22), confirming the significance of this gene in mediating protective immunity and in inducing strong innate and adaptive immune responses. It was also recently reported that the YF17D virus activates DCs by triggering their TLR2, 7, 8, and 9 (23). Our data reveal that TLR7 and its downstream adaptor molecule Myd88 are both up-regulated upon vaccination with YF17D. TLR7 is a molecular sensor for single-stranded RNA, such as the nucleic acid found in YF17D and other flaviviruses, and triggering of TLR7 causes the transduction of a signal, via Myd88, to up-regulate expression of inflammatory cytokines such as IL-6, IL-12, and TNF (via NF- κ B) and type I IFNs (via IRF7) (22, 24). Type I IFNs in turn enhance the expression of proteins with direct antiviral activity, such as ISG20 and OAS1, 2, and 3, which lead to viral RNA degradation, and MX1, MX2, ADAR, and EIF2AK2, which inhibit viral replication. We are showing that all these genes are up-regulated upon YF17D vaccination.

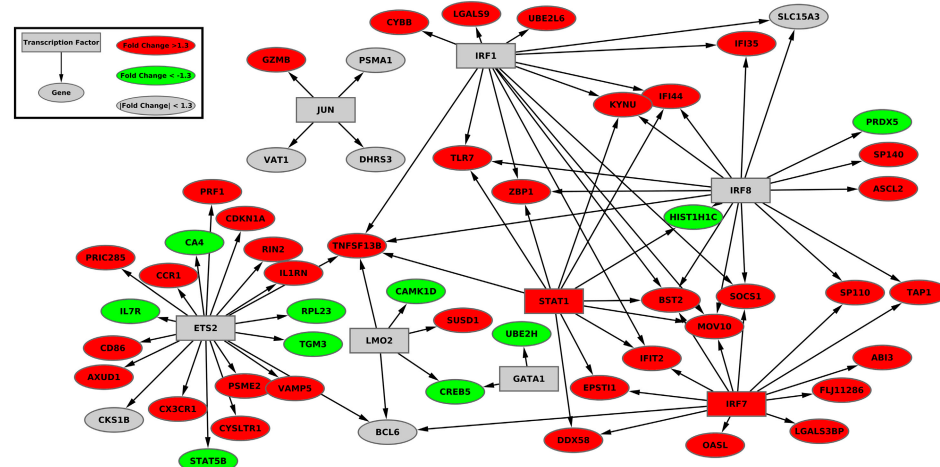


Figure 9. Consensus transcriptional network of genes differentially expressed on day 7 as compared with day 0. Network representation of inferred transcription factors and predicted target genes that are consistently modulated in at least two out of three datasets, with the third dataset not being contradictory.

Another prominent node of transcription regulation induced by YF17D vaccination is the ETS2 transcription factor. ETS2 is involved in the differentiation and maturation of several immune cell types (25). Its expression is up-regulated in activated and proliferating T cells (26) and ETS2 is involved in IL-12 p40 (Th1) and IL-5 (Th2) gene expression (27, 28). ETS2 obviously plays a key role in the highly integrated response to YF17D, as it enhanced transcription of several downstream genes that play critical roles in the maturation and differentiation of T cells, B cells, NK cells, and macrophages (Fig. 2, Fig. 3, and Fig. S1). Indeed, antigen-presenting cell-specific genes that are targets of ETS2 were up-regulated early after vaccination (MARCO, CD86). The role of ETS2 in the early induction of innate immunity is further demonstrated by the increased expression of NK cell receptors, as well as several cytolytic molecules; KIRDL3, PRF1, and GZMB are known targets of members of the Ets family of transcription factors (25, 29). Moreover, flow cytometry analysis on PBMCs from vaccinated volunteers revealed that YF17D stimulates the proliferation of several leukocyte populations (Fig. S5 b).

Several of the other predicted transcription nodes are likely to play significant roles in the induction of innate and adaptive immunity in response to YF17D. IRF1 mediates the antiviral activity of IFNs, similar to IRF7 (30). IRF1 and IRF8 were found to synergistically activate IL-12 p35 and p40 gene expression in macrophages (31–33). IRF8 also mediates activation of NF- κ B upon TLR9 triggering in DCs (34), and IRF8 and LMO2 were both found to be expressed in B cell germinal centers, suggesting a role in the development of the humoral response (35, 36). Moreover, TAL1 may be involved in T cell proliferation and differentiation (37). E2F4 is involved in cell cycle regulation (38), and FOXO3A and E2F1 are mediators of apoptosis (39, 40).

A common feature of these masterswitch genes is that they control the induction of several pathways of the innate immune response, including type I IFNs, but also the inflammasome and complement. The inflammasome is a large protein assembly that includes pyrin- and CARD domain-containing adaptor proteins complexed with cysteine proteinases known as caspases. It mediates the processing and activation of these caspases, and subsequently the cleavage and secretion of the proinflammatory cytokines IL-1 β and -18 (41). Activation of the inflammasome has been recently shown to be induced by adenoviruses (42), and to be a key event for the successful adjuvant effect of alum, one of the only two adjuvants licensed to be used in humans (43). Our gene array results demonstrate that two components of the inflammasome, caspase-1 and -5, were up-regulated after YF17D vaccination, in volunteers from the Montreal cohort, whereas only caspase-1 is up-regulated in volunteers from the Lausanne cohort (Fig. 5 a). There are different kinds of inflammasomes, each containing a specific combination of inflammatory caspases and adaptor molecules (44). Hence, NALP1 inflammasomes contain ASC, NALP1, caspase-1, and caspase-5, whereas NALP3 inflammasomes contain ASC, NALP3, and caspase-1 (no caspase-5).

It is possible that NALP1 inflammasomes were not induced in volunteers from the Lausanne cohort, whereas NALP3 inflammasomes were induced in both cohorts. Interestingly, our gene array data also show a modulation of genes that are involved in IL-1 β signaling, IL-1R2 and IL-1RN. IL-1R2, which is a decoy receptor that competes with the binding of IL-1 β to its receptor (45), is down-regulated, further confirming increased inflammasome activities and IL-1 β processing and secretion after immunization with YF17D. The gene encoding IL-1RN, a cytokine that is an IL-1R antagonist, is up-regulated upon vaccination; this increase could be part of a negative feedback loop or could be caused by the up-regulation of STAT1 and STAT2, two transcription factors that induce IL-1RN up-regulation (46, 47). Activation of the inflammasome by YF17D was confirmed at the protein level by incubating immature DCs with the virus and assessing their IL-1 β secretion. Representative results of ex vivo experiments performed on cells from a minimum of three individuals are shown in Fig. 5 b and Fig. S4, and clearly validate the gene expression data, as we could observe a significant up-regulation (up to ninefold) of IL-1 β , which is a critical indicator of inflammasome formation and activation. Of note, we could also observe that the induction of this pathway was independent of viral replication, as both UV-inactivated virus, and to a lesser extent heat-inactivated virus, all induced the secretion of IL-1 β . As shown in Fig. 5 a, the modulation of inflammasome- and IL-1 β -related genes also similarly occurred in the Lausanne cohort, where increased gene expression of caspase-1, IL-1RN, and the decrease in the expression of IL-1R2, further confirmed the activation of the inflammasome after YF17D vaccination. Altogether, these results confirm the importance of the inflammasome as a target of the YF17D vaccine. Whether this pathway is critical for the adjuvant effect of this vaccine remains to be determined, but is certainly suggested by the fact that the inflammasome is induced by immunization when alum is used as adjuvant (43). Moreover, IL-1 β is known to play an important role in the regulation of T cell activation at multiple levels, and polymorphisms in the IL-1 β gene have been linked to smallpox vaccine-induced fever (48).

We observed that YF17D stimulated the up-regulation of components of the complement cascade in blood cells, namely C1qA and C1qB. These molecules have been shown to induce maturation of DCs (49). Furthermore, distinct components of the complement pathway were found to be essential in the development of humoral and cellular immunity to another flavivirus, the West Nile Virus (50, 51). This may underline a possible role for the complement system in the establishment of immunity in response to YF17D vaccination.

The induction of a mixed Th1/Th2 profile by YF17D was suggested by Querec et al., who reported that the vaccine triggers TLR2, 7, 8, and 9 on DCs (23); this was recently confirmed with in vivo data in humans (52). Our results corroborate these findings; we have demonstrated at the protein level that PBMCs isolated from YF17D-vaccinated volunteers display a mixed T helper cell phenotype. Cells from day

60 post-vaccination subjects, when stimulated ex vivo with YF17D-derived peptides, secreted Th1 and Th2 cytokines in their supernatants, as measured by CBA (Fig. 6 and Fig. S6 e). Peptide-stimulated PBMCs from day 28 expressed the Th1 cytokines IL-2 and/or IFN- γ , as revealed by intracellular cytokine staining (Fig. 7 a), and finally, PBMCs from day 365 after vaccination contained central memory T helper cells expressing surface markers typical of Th1 or Th2 cells when stimulated twice with immunostimulatory YF17D peptide pools (Fig. 7 b). Induction of the Th2 pathway by a vaccine is essential for the development of humoral immunity; in that context, we noted the induction of several B cell-specific genes in whole blood from volunteers vaccinated with YF17D, including POU2AF1, a transcription factor that is essential for mature B cell differentiation (53), and CD19, TNFRSF13B (BAFF) and TNFRSF17 (BCMA; Fig. 3 e), which are critical for B cell survival, persistence, and isotype switching (54). This late induction of B cell-associated genes (days 10 and 14) coincided with the onset of YF17D-specific neutralizing antibody production, which occurred by day 14 in the majority of the vaccinated volunteers (Table S2).

The MIMIC system confirmed that the YF17D vaccine can induce a mixed Th1/Th2 response, as measured by the secretion of the Th1 cytokines IL-2 and IFN- γ , and the Th2 cytokines IL-5 and -13 in the supernatants of the MIMIC co-cultures (Fig. 8 c), and by the production of IL-5 and -13 (Fig. 8 b) or IFN- γ (Fig. 8 a) by antigen-specific CD154 $^+$ T helper cells. The observation that both live and UV-inactivated YF17D virus stimulate an identical response clearly shows that viral replication is not required for the induction of adaptive immunity. Importantly, we show by gene array that most of the transcriptional nodes involved in the response to YF17D in vivo that were identified with the Montreal cohort (Fig. 2) are also induced in the Lausanne cohort, as well as in the in vitro MIMIC system (Table S3), leading to the mobilization of several of their downstream transcriptional targets. Specifically, we found that immunization with YF17D elicits the induction of IRF1, IRF7, IRF8, STAT1, and FOXO3a in all three datasets, all of which are master-switch genes required for the coordination of an efficient and protective immune response. Moreover, ICA followed by gene set enrichment (Table S4, available at <http://www.jem.org/cgi/content/full/jem.20082292/DC1>) has revealed a significant enrichment of genes induced by IFNs and viruses among the three datasets, namely those from Montreal, Lausanne, and VaxDesign's MIMIC system.

Our results highlight the critical role of innate immunity in the elicitation of the multilineage and broad immune responses observed herein, and demonstrate the complexity of the innate immune response that is generated upon vaccination with YF17D. Indeed, several effector molecules of the innate immune response, including complement, IFNs, the inflammasome, and several effector cells of innate immunity (i.e., macrophages, NK cells, and DCs, the latter being most likely the producers of type I IFNs [55]), are involved in this early response (day 3 and 7). Control of viral replication

(Table S5, available at <http://www.jem.org/cgi/content/full/jem.20082292/DC1>) happens as this innate response precedes the emergence of YF17D-specific humoral and cellular immune responses. Interestingly, complement, IFNs, and the inflammasome can all impact on the quality of the adaptive immune response and trigger Th1/Th2 mixed immune responses (42). Notably, YF17D triggers TLR2, which is upstream of the Th2 pathway (56) and TLR7, 8, and 9, which trigger mostly the Th1 pathway (57). Our studies have also revealed that the mixed Th1/Th2 CD4 $^+$ response preceded B cell responses, as monitored by the detection of antibodies in serum of vaccinated subjects and the identification of gene expression signatures specific to B cell responses (Table S2 and Fig. 3 e). An important outcome of the early development of Th2 memory CD4 $^+$ T cells is the generation and persistence of a strong antibody response. As for CD8 $^+$ responses, they could certainly be involved in providing long-lasting protection against reexposure to the virus. In that context, it will be important to compare the immune response described herein to that of individuals that have been reexposed to the virus, such as those who live in endemic areas or who get reimmunized with the vaccine.

The results described herein identify unique features of protective immune responses which can now be used as benchmarks to design and monitor the development of novel vaccines. They demonstrate the complexity of this immune response and they highlight the fact that it is the sum of all arms of the immune response that is most probably required for the long-lasting protection induced by this vaccine; and they highlight the fact that it is this integrated immune response that constitutes the correlates of protection. In that context, systems biology becomes an essential tool to identify correlates of immune-mediated protection. The recent failure of the STEP HIV vaccine trial paves the way for the use of new immune monitoring strategies focused on the identification of multilineage and polyfunctional features of candidate vaccine-induced immune response.

MATERIALS AND METHODS

Vaccination of human volunteers and blood collection. The volunteer recruitment and vaccination protocols for this study were approved by the research ethics committees of the Centre Hospitalier de l'Université de Montréal (Montreal cohort; 20 volunteers), the Faculty of Biology and Medicine of the University of Lausanne (Lausanne cohort; 13 volunteers), and Emory University (Emory Cohort; 10 volunteers). Each recruited subject received a single 0.5-ml subcutaneous injection of the Sanofi-Pasteur 17D-204 live-attenuated YF virus vaccine YF-VAX (Montreal and Emory cohorts) or Stamaril (Lausanne cohort). For the Montreal cohort, 50 ml of blood were drawn from each volunteer in sodium-heparinized Vacutainer tubes (BD) on the day of vaccination (day 0) and 3, 7, 10, 14, 28, 60, 90, 180, and 365 d thereafter. PBMCs were isolated from these samples using standard Ficoll-Paque Plus (GE Healthcare) density gradient centrifugation and cryopreserved in bovine serum + 10% DMSO in liquid nitrogen. At each time point, an additional 10 ml of blood was collected from each volunteer in PaxGene tubes (QIAGEN), for whole-blood RNA isolation. For the Lausanne cohort, whole blood was collected in PaxGene tubes at days 0, 3, and 7 after vaccination. YF17D-specific seroconversion and viremia were determined as described in Tables S2 and S5, respectively.

Gene array analysis of whole-blood and VaxDesign samples. Whole-blood total RNA was purified from PaxGene tubes using RNA extraction kits (QIAGEN). Quantification was performed using a spectrophotometer (NanoDrop Technologies) and RNA quality was assessed using the Experion automated electrophoresis system (Bio-Rad Laboratories). Total RNA was then amplified and labeled using the Illumina TotalPrep RNA Amplification kit, which is based on the Eberwine amplification protocol (58). This protocol involves a first cDNA synthesis step followed by *in vitro* transcription for cRNA synthesis. The biotinylated cRNA was hybridized onto Illumina Human RefSeq-8 BeadChips v2 (Montreal and Lausanne samples) or v3 (VaxDesign samples) at 58°C for 20 h and quantified using Illumina BeadStation 500GX scanner and Illumina BeadStudio v3 software.

Illumina probe data were exported from BeadStudio as raw data and screened for quality. Samples failing chip visual inspection and control examination were removed. Gene expression data were analyzed using Bioconductor (59), an open-source software library for the analyses of genomic database on R, which is a language and environment for statistical computing and graphics (www.r-project.org). The R software package was used to first filter out probes with intensities below background in all samples, and then to minimum replace (a surrogate replacement policy) values below background using the mean background value of the built-in Illumina probe controls as an alternative to background subtraction (which may introduce negative values) to reduce “overinflated” expression ratios determined in subsequent steps, and finally quantile normalize the probe intensities. The resulting matrix showing probes as rows and samples as columns was log₂ transformed and used as input for linear modeling using BioConductor Linear models for microarray analysis (LIMMA [60]). The LIMMA package (61) was used to identify differentially expressed genes (pFDR <0.05; fold change greater than -1.3 or >1.3) at days 3, 7, 10, 14, 28, and 60, compared with day 0 for the Montreal samples, at days 3 and 7 compared with day 0 for the Lausanne samples, and at days 3 and 7 compared with the respective control for the VaxDesign samples. Our microarray data are available through the National Center for Biotechnology Information Gene Expression Omnibus (GEO) under series accession no. GSE13699.

qPCR validation. Changes in gene expression observed by microarray analyses were verified by qPCR. The expression of 43 genes, which were chosen according to our microarray results and to biomedical literature, was analyzed on samples obtained at day 0 and 7 after vaccination from the Montreal and Lausanne cohorts. To further validate our microarray data, we also performed qPCR analysis on RNA samples (day 0 and 7) from 10 YF17D-vaccinated volunteers enrolled in another vaccination trial conducted by the Emory Vaccine Center in Atlanta, GA (a gift from B. Pulendran). qPCR analysis was performed at the genomics platform of the Institute for Research in Immunology and Cancer (Montreal), as previously described (62).

Identification of transcription factors and curated gene sets. Transcription factors were identified using ICA and gene set enrichment as described in Teschendorff et al. (63). ICA was performed on the expression profiles of the whole-blood and ex vivo model gene arrays (Montreal, Lausanne, and VaxDesign) on each day individually, as well as on the whole datasets from each study. The CRAN package fastICA (v1.1-9) was used to carry out the ICA. Genes in each component were chosen for enrichment by selecting genes with loads below the 2.fifth percentile or above the 97.fifth percentile. Gene set enrichment was done on the C2 “curated gene sets” and C3 “motif gene sets” collections of MsigDB. The resulting P values were Benjamini-Hochberg adjusted to keep the false discovery rates within each component <5%. Results annotated with unknown transcription factors that were discarded. Additionally, at least one gene in the gene sets used for enrichment had to be differentially expressed (see Gene array analysis of whole blood and VaxDesign samples) on at least one of the available time points up to day 14.

In vitro infection of immature DCs with YF17D. Stocks of live YF17D virus were prepared in our laboratory by infecting Vero cell monolayers grown in DME medium (Sigma-Aldrich) supplemented with 10% X-

Vivo 15 medium (Lonza), with YF17D, and harvesting the culture supernatants when severe histopathology could be observed (6–7 d). The virus particles were concentrated using Centricon Plus-20 columns (100 kD cutoff; Millipore). Viral stocks were titrated on Vero cells by lysis plaque assay. The virus was either heat-inactivated by incubation at 65°C for 1 h, or UV-inactivated at a dose of 0.72 J/cm² in a Stratalinker 1800 (Stratagene). Inactivated YF17D was tested by plaque assay to ensure total inactivation.

Immature DCs were generated by culturing monocytes for 6 d in the presence of 100 ng/ml GM-CSF (R&D Systems) and 25 ng/ml IL-4 (R&D Systems). The cells were then incubated with live, UV-inactivated or heat-inactivated YF17D, at a multiplicity of infection of 10. After 24 and 48 h, supernatants were collected and analyzed using an IL-1 β ELISA kit (BD).

Proliferation and cytokine secretion assays. PBMCs from vaccinated volunteers were labeled with CFSE (Invitrogen), as previously described (64). 2 million cells were incubated in polypropylene snap-cap tubes (Falcon) in the presence of YF17D-derived peptide pools (Fig. S6 a) at a final concentration of 2 μ g/ml/peptide, SEB (50 ng/ml; Toxin Technology) or nothing (nonstimulated; NS). After 24 h of incubation at 37°C/5% CO₂, 120 μ l of supernatant was withdrawn from each tube and frozen at -80°C for subsequent cytokine analysis. The same volume of fresh medium was replaced in each tube, and 5 d later (6 d total incubation), the cells were harvested and stained with anti-CD3, -CD4, and -CD8 antibodies (BD). The cells were collected on a BD LSRII flow cytometer and the results were analyzed using the BD FACSDiva software. The BD Th1/Th2 CBA array (BD) was used to measure levels of IL-2, IL-4, IL-5, IL-10, IFN- γ , and TNF in PBMCs supernatants, as suggested by the manufacturer.

Flow cytometric analysis of IFN- γ /IL-2-producing activated CD4 T cells. To assess the cytokine production ability of YF17D-specific helper T cells, 2 million PBMCs from vaccinated subjects (day 14 and 28) were stimulated for 6 h with YF17D-derived peptide pools, in the presence of Brefeldin A (Sigma-Aldrich), and then stained with anti-CD8 and -CD4 antibodies. They were then permeabilized and stained with anti-CD154, IL-2, and IFN- γ (BD).

To determine the T helper phenotype of long-term, vaccine-specific CD4 $^{+}$ T cells, 2 million PBMCs were stimulated for 6 d with YF17D peptide pools, and subsequently restimulated with the same pools for 12 h, in the presence of Brefeldin A. Non-restimulated cells were used as controls. The cells were then stained with anti-CD3, -CD4, -CD8, -CD45RA, -CCR7, -CCR4, -CXCR3, and -CCR6 antibodies (BD). After permeabilization, they were stained for intracellular CD154 and fixed.

The MIMIC co-culture system. PBMCs used in the assays were acquired from normal healthy donors enrolled in a VaxDesign Corporation apheresis study program (protocol CRRI 0906009). Blood collections were performed at Florida’s Blood Centers (Orlando, FL) using standard techniques. The enriched leukocytes were isolated and cryopreserved. Human DCs were prepared as described above. After 5 d of culture with IL-4 and GM-CSF, the DCs were infected with a 1:100 dilution of the live-attenuated YF-VAX vaccine. After 24 h, 5% human AB serum was added to the media to quench the infection. Alternatively, some of the DCs were pulsed with a 1:100 dilution of YF-VAX (YF) that had been UV-inactivated. On the sixth day, all DCs were matured with an overnight treatment of 25 ng/ml TNF- α (R&D Systems).

CD4 $^{+}$ T cell stimulation assay. Frozen stocks of autologous PBMCs were used as a source of lymphocytes. Purified CD4 $^{+}$ T cells were co-cultured with untreated or YF17D-pulsed DCs at a ratio of 60:1 for 14 d; thereafter, the activated lymphocytes were harvested and evaluated for effector activity using autologous DCs as APCs. The T cells and APCs were co-cultured for 7 h, stained with CD4 antibody, permeabilized, and labeled intracellularly with anti-IFN- γ , -IL-5, -IL-13, and -CD154 antibodies.

Multiplex cytokine analysis. At the time the lymphocytes were harvested from DC/T cell co-cultures, the supernatants were also collected and stored

frozen until analyzed for cytokine production using the Beadlyte human 22-plex Multi-cytokine Detection System (Millipore) on a Bio-Plex reader (Bio-Rad Laboratories).

Online supplemental materials. Fig. S1 shows the transcriptional network of differentially expressed genes after YF17D vaccination, as inferred by gene set enrichment. Fig. S2 shows the correlation of gene expression between Illumina array and qPCR data (Montreal cohort). Fig. S3 shows a heat map of fold change gene expression (all 43 genes tested) between day 0 and day 3 or 7 after YF17D vaccination, as measured by qPCR. Fig. S4 shows the production of IL-1 β by DCs in response to YF17D. Fig. S5 shows the expression of Ki67 by different subsets of PBMCs after YF17D vaccination. Fig. S6 shows the induction of antigen-specific CD4 $^{+}$ and CD8 $^{+}$ T cell responses by YF17D vaccination. Fig. S7 shows the gating strategy used to identify central memory Th1 and Th2 cells by flow cytometry. Table S1 shows the results of qPCR analysis of RNA samples from three independent YF17D vaccination studies. Table S2 shows the neutralizing humoral immune response elicited by the YF17D vaccine in the Montreal cohort. Table S3 shows a comparison between the transcription factors induced by YF17D in the Montreal cohort, the Lausanne cohort, and VaxDesign's MIMIC system. Table S4 shows the induction by YF17D of Common gene sets in the Montreal, Lausanne, and VaxDesign microarray data. Table S5 shows the development of viremia after vaccination with YF17D. Document S1 shows the list of significant genes modulated after YF17D vaccination. Document S2 shows the lists of genes selected to make up the different gene sets used for Figs. 3 and 5 a. These lists were derived from published literature. Online supplemental material is available at <http://www.jem.org/cgi/content/full/jem.20082292/DC1>.

We thank M. Lainesse and R. Bordi for expert technical assistance. YF-VAX was generously provided by Sanofi Pasteur. We thank Dr. Bali Pulendran for giving us the Emory vaccine trial samples. We are grateful to Drs. B. Genton and S. de Vallière for protocol discussion and support in the recruitment of volunteers from Lausanne.

This study was supported by funds from Genome Canada, Genome Québec, the Canadian Network for Vaccines and Immunotherapeutics (CANVAC), the Institut National de la Santé et de la Recherche Médicale (INSERM), and the IAVI Innovation Fund. R.P. Sekaly is the Canada Research Chair in Human Immunology. D. Gaucher is the recipient of a postdoctoral fellowship from the "Fonds de la recherche en santé du Québec". R. Therrien is supported by a scholarship from INSERM.

The authors have no conflicting financial interest.

Submitted: 14 October 2008

Accepted: 20 November 2008

REFERENCES

1. Sekaly, R.P. 2008. The failed HIV Merck vaccine study: a step back or a launching point for future vaccine development? *J. Exp. Med.* 205:7–12.
2. Plotkin, S., and W. Orenstein. 2004. Vaccines. WB Saunders, Philadelphia.
3. McMichael, A.J. 2006. HIV vaccines. *Annu. Rev. Immunol.* 24:227–255.
4. Monath, T.P. 2004. Yellow fever vaccine. In *Vaccines*. S. Plotkin and W. Orenstein, editors. WB Saunders, Philadelphia. 1095–1176.
5. Bauer, J.H. 1931. The duration of passive immunity in yellow fever. *Am. J. Trop. Med. Hyg.* 11:451.
6. Brandriss, M.W., J.J. Schlesinger, E.E. Walsh, and M. Briselli. 1986. Lethal 17D yellow fever encephalitis in mice. I. Passive protection by monoclonal antibodies to the envelope proteins of 17D yellow fever and dengue 2 viruses. *J. Gen. Virol.* 67(Pt 2):229–234.
7. Reinhardt, B., R. Jaspert, M. Niedrig, C. Kostner, and J. L'Age-Stehr. 1998. Development of viremia and humoral and cellular parameters of immune activation after vaccination with yellow fever virus strain 17D: a model of human flavivirus infection. *J. Med. Virol.* 56:159–167.
8. Santos, A.P., A.L. Bertho, D.C. Dias, J.R. Santos, and R. Marcovitz. 2005. Lymphocyte subset analyses in healthy adults vaccinated with yellow fever 17DD virus. *Mem. Inst. Oswaldo Cruz.* 100:331–337.
9. Co, M.D., M. Terajima, J. Cruz, F.A. Ennis, and A.L. Rothman. 2002. Human cytotoxic T lymphocyte responses to live attenuated 17D yel-
- low fever vaccine: identification of HLA-B35-restricted CTL epitopes on nonstructural proteins NS1, NS2b, NS3, and the structural protein E. *Virology.* 293:151–163.
10. Miller, J.D., R.G. van der Most, R.S. Akondy, J.T. Glidewell, S. Abbott, D. Masopust, K. Murali-Krishna, P.L. Mahar, S. Edupuganti, S. Lalor, et al. 2008. Human effector and memory CD8 $^{+}$ T cell responses to smallpox and yellow fever vaccines. *Immunity.* 28:710–722.
11. Xie, X., J. Lu, E.J. Kulkoski, T.R. Golub, V. Mootha, K. Lindblad-Toh, E.S. Lander, and M. Kellis. 2005. Systematic discovery of regulatory motifs in human promoters and 3' UTRs by comparison of several mammals. *Nature.* 434:338–345.
12. Monaco, J.J., S. Cho, and M. Attaya. 1990. Transport protein genes in the murine MHC: possible implications for antigen processing. *Science.* 250:1723–1726.
13. Trowsdale, J., I. Hanson, I. Mockridge, S. Beck, A. Townsend, and A. Kelly. 1990. Sequences encoded in the class II region of the MHC related to the 'ABC' superfamily of transporters. *Nature.* 348:741–744.
14. Nicholson, S.E., and D.J. Hilton. 1998. The SOCS proteins: a new family of negative regulators of signal transduction. *J. Leukoc. Biol.* 63:665–668.
15. Scherer, C.A., C.L. Magness, K.V. Steiger, N.D. Poitinger, C.M. Caputo, D.G. Miner, P.L. Winokur, D. Klinzman, J. McKee, C. Pilar, et al. 2007. Distinct gene expression profiles in peripheral blood mononuclear cells from patients infected with vaccinia virus, yellow fever 17D virus, or upper respiratory infections. *Vaccine.* 25:6458–6473.
16. Martinon, F., K. Burns, and J. Tschoopp. 2002. The inflammasome: a molecular platform triggering activation of inflammatory caspases and processing of proIL-beta. *Mol. Cell.* 10:417–426.
17. Chattopadhyay, P.K., J. Yu, and M. Roederer. 2005. A live-cell assay to detect antigen-specific CD4 $^{+}$ T cells with diverse cytokine profiles. *Nat. Med.* 11:1113–1117.
18. Frentschi, M., O. Arbach, D. Kirchhoff, B. Moewes, M. Worm, M. Rothe, A. Scheffold, and A. Thiel. 2005. Direct access to CD4 $^{+}$ T cells specific for defined antigens according to CD154 expression. *Nat. Med.* 11:1118–1124.
19. Rivino, L., M. Messi, D. Jarrossay, A. Lanzavecchia, F. Sallusto, and J. Geginat. 2004. Chemokine receptor expression identifies Pre-T helper (Th1), Pre-Th2, and nonpolarized cells among human CD4 $^{+}$ central memory T cells. *J. Exp. Med.* 200:725–735.
20. Poland, J.D., C.H. Calisher, T.P. Monath, W.G. Downs, and K. Murphy. 1981. Persistence of neutralizing antibody 30–35 years after immunization with 17D yellow fever vaccine. *Bull. World Health Organ.* 59:895–900.
21. Colina, R., M. Costa-Mattioli, R.J. Dowling, M. Jaramillo, L.H. Tai, C.J. Breitbach, Y. Martineau, O. Larsson, L. Rong, Y.V. Svitkin, et al. 2008. Translational control of the innate immune response through IRF-7. *Nature.* 452:323–328.
22. Honda, K., H. Yanai, H. Negishi, M. Asagiri, M. Sato, T. Mizutani, N. Shimada, Y. Ohba, A. Takaoka, N. Yoshida, and T. Taniguchi. 2005. IRF-7 is the master regulator of type-I interferon-dependent immune responses. *Nature.* 434:772–777.
23. Querec, T., S. Bennouna, S. Alkan, Y. Laouar, K. Gorden, R. Flavell, S. Akira, R. Ahmed, and B. Pulendran. 2006. Yellow fever vaccine YF-17D activates multiple dendritic cell subsets via TLR2, 7, 8, and 9 to stimulate polyvalent immunity. *J. Exp. Med.* 203:413–424.
24. Kawai, T., and S. Akira. 2006. TLR signaling. *Cell Death Differ.* 13:816–825.
25. Gallant, S., and G. Gilkeson. 2006. ETS transcription factors and regulation of immunity. *Arch. Immunol. Ther. Exp. (Warsz.).* 54:149–163.
26. Bhat, N.K., C.B. Thompson, T. Lindsten, C.H. June, S. Fujiwara, S. Koizumi, R.J. Fisher, and T.S. Papas. 1990. Reciprocal expression of human ETS1 and ETS2 genes during T-cell activation: regulatory role for the protooncogene ETS1. *Proc. Natl. Acad. Sci. USA.* 87:3723–3727.
27. Sun, H.J., X. Xu, X.L. Wang, L. Wei, F. Li, J. Lu, and B.Q. Huang. 2006. Transcription factors Ets2 and Sp1 act synergistically with histone acetyltransferase p300 in activating human interleukin-12 p40 promoter. *Acta Biochim. Biophys. Sin. (Shanghai).* 38:194–200.
28. Blumenthal, S.G., G. Aichele, T. Wirth, A.P. Czernilofsky, A. Nordheim, and J. Dittmer. 1999. Regulation of the human interleukin-5 promoter by Ets transcription factors. Ets1 and Ets2, but not

- Elf-1, cooperate with GATA3 and HTLV-I Tax1. *J. Biol. Chem.* 274:12910–12916.
29. Koizumi, H., M.F. Horta, B.S. Youn, K.C. Fu, B.S. Kwon, J.D. Young, and C.C. Liu. 1993. Identification of a killer cell-specific regulatory element of the mouse perforin gene: an Ets-binding site-homologous motif that interacts with Ets-related proteins. *Mol. Cell. Biol.* 13:6690–6701.
 30. Harada, H., T. Taniguchi, and N. Tanaka. 1998. The role of interferon regulatory factors in the interferon system and cell growth control. *Biochimie.* 80:641–650.
 31. Masumi, A., S. Tamaoki, I.M. Wang, K. Ozato, and K. Komuro. 2002. IRF-8/ICSBP and IRF-1 cooperatively stimulate mouse IL-12 promoter activity in macrophages. *FEBS Lett.* 531:348–353.
 32. Wang, I.M., C. Contursi, A. Masumi, X. Ma, G. Trinchieri, and K. Ozato. 2000. An IFN-gamma-inducible transcription factor, IFN consensus sequence binding protein (ICSBP), stimulates IL-12 p40 expression in macrophages. *J. Immunol.* 165:271–279.
 33. Liu, J., X. Guan, T. Tamura, K. Ozato, and X. Ma. 2004. Synergistic activation of interleukin-12 p35 gene transcription by interferon regulatory factor-1 and interferon consensus sequence-binding protein. *J. Biol. Chem.* 279:55609–55617.
 34. Tsujimura, H., T. Tamura, H.J. Kong, A. Nishiyama, K.J. Ishii, D.M. Klinman, and K. Ozato. 2004. Toll-like receptor 9 signaling activates NF-kappaB through IFN regulatory factor-8/IFN consensus sequence binding protein in dendritic cells. *J. Immunol.* 172:6820–6827.
 35. Lee, C.H., M. Melchers, H. Wang, T.A. Torrey, R. Slota, C.F. Qi, J.Y. Kim, P. Lugar, H.J. Kong, L. Farrington, et al. 2006. Regulation of the germinal center gene program by interferon (IFN) regulatory factor 8/IFN consensus sequence-binding protein. *J. Exp. Med.* 203:63–72.
 36. Natkunam, Y., S. Zhao, D.Y. Mason, J. Chen, B. Taidi, M. Jones, A.S. Hammer, S. Hamilton Dutoit, I.S. Losso, and R. Levy. 2007. The oncogene LMO2 is expressed in normal germinal-center B cells and in human B-cell lymphomas. *Blood.* 109:1636–1642.
 37. Hansson, A., C. Manetopoulos, J.I. Jonsson, and H. Axelson. 2003. The basic helix-loop-helix transcription factor TAL1/SCL inhibits the expression of the p16INK4A and pTalpha genes. *Biochem. Biophys. Res. Commun.* 312:1073–1081.
 38. Sardet, C., M. Vidal, D. Cobrinik, Y. Geng, C. Onufryk, A. Chen, and R.A. Weinberg. 1995. E2F-4 and E2F-5, two members of the E2F family, are expressed in the early phases of the cell cycle. *Proc. Natl. Acad. Sci. USA.* 92:2403–2407.
 39. van Grevenynghe, J., F.A. Procopio, Z. He, N. Chomont, C. Riou, Y. Zhang, S. Gimmig, G. Boucher, P. Wilkinson, Y. Shi, et al. 2008. Transcription factor FOXO3a controls the persistence of memory CD4(+) T cells during HIV infection. *Nat. Med.* 14:266–274.
 40. Furukawa, Y., N. Nishimura, M. Satoh, H. Endo, S. Iwase, H. Yamada, M. Matsuda, Y. Kano, and M. Nakamura. 2002. Apaf-1 is a mediator of E2F-1-induced apoptosis. *J. Biol. Chem.* 277:39760–39768.
 41. Petrilli, V., C. Dostert, D.A. Muruve, and J. Tschopp. 2007. The inflammasome: a danger sensing complex triggering innate immunity. *Curr. Opin. Immunol.* 19:615–622.
 42. Muruve, D.A., V. Petrilli, A.K. Zaiss, L.R. White, S.A. Clark, P.J. Ross, R.J. Parks, and J. Tschopp. 2008. The inflammasome recognizes cytosolic microbial and host DNA and triggers an innate immune response. *Nature.* 452:103–108.
 43. Li, H., S.B. Willingham, J.P. Ting, and F. Re. 2008. Cutting edge: inflammasome activation by alum and alum's adjuvant effect are mediated by NLRP3. *J. Immunol.* 181:17–21.
 44. Martinon, F., and J. Tschopp. 2004. Inflammatory caspases: linking an intracellular innate immune system to autoinflammatory diseases. *Cell.* 117:561–574.
 45. Mantovani, A., M. Locati, A. Vecchi, S. Sozzani, and P. Allavena. 2001. Decoy receptors: a strategy to regulate inflammatory cytokines and chemokines. *Trends Immunol.* 22:328–336.
 46. Wan, L., C.W. Lin, Y.J. Lin, J.J. Sheu, B.H. Chen, C.C. Liao, Y. Tsai, W.Y. Lin, C.H. Lai, and F.J. Tsai. 2008. Type I IFN induced IL1-Ra expression in hepatocytes is mediated by activating STAT6 through the formation of STAT2: STAT6 heterodimer. *J. Cell. Mol. Med.* 12:876–878.
 47. Gabay, C., M. Dreyer, N. Pellegrinelli, R. Chicheportiche, and C.A. Meier. 2001. Leptin directly induces the secretion of interleukin 1 receptor antagonist in human monocytes. *J. Clin. Endocrinol. Metab.* 86:783–791.
 48. Stanley, S.L. Jr., S.E. Frey, P. Taillon-Miller, J. Guo, R.D. Miller, D.C. Koboldt, M. Elashoff, R. Christensen, N.L. Saccone, and R.B. Belshe. 2007. The immunogenetics of smallpox vaccination. *J. Infect. Dis.* 196:212–219.
 49. Csomor, E., Z. Bajtay, N. Sandor, K. Kristof, G.J. Arlaud, S. Thiel, and A. Erdei. 2001. Complement protein C1q induces maturation of human dendritic cells. *Mol. Immunol.* 44:3389–3397.
 50. Mehlhop, E., and M.S. Diamond. 2006. Protective immune responses against West Nile virus are primed by distinct complement activation pathways. *J. Exp. Med.* 203:1371–1381.
 51. Mehlhop, E., K. Whitby, T. Oliphant, A. Marri, M. Engle, and M.S. Diamond. 2005. Complement activation is required for induction of a protective antibody response against West Nile virus infection. *J. Virol.* 79:7466–7477.
 52. Santos, A.P., D.C. Matos, A.L. Bertho, S.C. Mendonca, and R. Marcovitz. 2008. Detection of Th1/Th2 cytokine signatures in yellow fever 17DD first-time vaccinees through ELISpot assay. *Cytokine.* 42:152–155.
 53. Brunner, C., A. Sindrilariu, I. Girkontaite, K.D. Fischer, C. Sunderkotter, and T. Wirth. 2007. BOB.1/OBF.1 controls the balance of TH1 and TH2 immune responses. *EMBO J.* 26:3191–3202.
 54. Wang, Y., and R.H. Carter. 2005. CD19 regulates B cell maturation, proliferation, and positive selection in the FDC zone of murine splenic germinal centers. *Immunity.* 22:749–761.
 55. Steinman, R.M., and J. Banchereau. 2007. Taking dendritic cells into medicine. *Nature.* 449:419–426.
 56. Redecke, V., H. Hacker, S.K. Datta, A. Fermin, P.M. Pitha, D.H. Broide, and E. Raz. 2004. Cutting edge: activation of Toll-like receptor 2 induces a Th2 immune response and promotes experimental asthma. *J. Immunol.* 172:2739–2743.
 57. Gorden, K.B., K.S. Gorski, S.J. Gibson, R.M. Kedl, W.C. Kieper, X. Qiu, M.A. Tomai, S.S. Alkan, and J.P. Vasilakos. 2005. Synthetic TLR agonists reveal functional differences between human TLR7 and TLR8. *J. Immunol.* 174:1259–1268.
 58. Van Gelder, R.N., M.E. von Zastrow, A. Yool, W.C. Dement, J.D. Barchas, and J.H. Eberwine. 1990. Amplified RNA synthesized from limited quantities of heterogeneous cDNA. *Proc. Natl. Acad. Sci. USA.* 87:1663–1667.
 59. Gentleman, R.C., V.J. Carey, D.M. Bates, B. Bolstad, M. Dettling, S. Dudoit, B. Ellis, L. Gautier, Y. Ge, J. Gentry, et al. 2004. Bioconductor: open software development for computational biology and bioinformatics. *Genome Biol.* 5:R80.
 60. Smyth, G.K. 2004. Linear models and empirical bayes methods for assessing differential expression in microarray experiments. *Stat. Appl. Genet. Mol. Biol.* 3.
 61. Smith, G.K. 2005. Limma: linear models for microarray data. In *Bioinformatics and Computational Biology Solutions using R and Bioconductor*. W. Huber, editor. Springer, New York. 397–420.
 62. Baron, C., R. Somogyi, L.D. Greller, V. Rineau, P. Wilkinson, C.R. Cho, M.J. Cameron, D.J. Kelvin, P. Chagnon, D.C. Roy, et al. 2007. Prediction of graft-versus-host disease in humans by donor gene-expression profiling. *PLoS Med.* 4:e23.
 63. Teschendorff, A.E., M. Journeé, P.A. Absil, R. Sepulchre, and C. Caldas. 2007. Elucidating the altered transcriptional programs in breast cancer using independent component analysis. *PLoS Comput. Biol.* 3:e161.
 64. Younes, S.A., B. Yassine-Diab, A.R. Dumont, M.R. Boulassel, Z. Grossman, J.P. Routy, and R.P. Sekaly. 2003. HIV-1 viremia prevents the establishment of interleukin 2-producing HIV-specific memory CD4+ T cells endowed with proliferative capacity. *J. Exp. Med.* 198:1909–1922.